Photochemistry and Photobiology, 1998, 68(4): 487–493

Kinetics and Mechanism of the Photosensitized Oxidation of Furosemide*

A. L. Zanocco†, G. Günther S., E. Lemp M., J. R. de la Fuente and N. Pizarro U.

Universidad de Chile, Departamento de Química Orgánica y Fisicoquímica, Santiago, Chile

Received 19 May 1998; accepted 17 July 1998

ABSTRACT

Detection of $O_2(^1\Delta_g)$ phosphorescence emission, λ_{max} = 1270 nm, following laser excitation and steady-state competitive methods was employed to measure total rate constants, k_T, for the reactions of the diuretic furosemide, 2-methylfurane and furfurylamine with singlet oxygen in several solvents. Correlation of k_T values with solvent parameters and product identification shows that the reaction mechanism is strongly solvent dependent. In aliphatic alcohols, the dependence of k_T on solvent parameters is similar to the one observed for triethylamine, suggesting a reaction mechanism involving partial charge transfer from the amino group to the singlet oxygen. In nonprotic solvents, the dependence of k_T on solvent parameters resembles the behavior found for 2-methylfurane and furfurylamine, implying that mostly a 2 + 4 cycloaddition mechanism of singlet oxygen to furane ring of furosemide occurs in these solvents. These mechanistic differences are explained in terms of hydrogen-bonding interactions between the carboxylic group in the aromatic ring and the amino group of furosemide. Furthermore, direct generation of $O_2(^1\Delta_g)$ by furosemide was detected. Quantum yields of 0.047 ± 0.003 and 0.078 ± 0.004 were determined in acetonitrile and benzene, respectively. This last result may be related, at least partially, to the photodynamic effects of this diuretic drug.

INTRODUCTION

Furosemide,‡ 4-chloro-*N*-furfuryl-5-sulfamoylanthranilic acid, is a widely used diuretic in the treatment of edema, which is administered both orally and parenterally. Previous studies have established that furosemide causes adverse photosensitivity effects *in vivo* (1) and has a high *in vitro* photosensitizing capability, being able to initiate both excited-state energy transfer reactions and free radical reactions (2,3). Several researchers have studied its photodegradation. Rowbotham *et al.* (4) reported that UV irradiation of furosemide in aqueous alkaline solutions produces 4-chloro-5-sulfoanthranilic acid by oxidation of the sulfamoyl group and hydrolysis of the furfuryl group, whereas Moore and Tamat (5) reported complete dechlorination of furosemide in deoxygenated neutral water. Irradiation of methanolic solutions of furosemide with 365 nm UV light induces two types of processes: photoreduction to give *N*-furfuryl-5-sulfamoylanthranilic acid and photosolvolysis to yield saluamine (6). Additionally, Bundgaard *et al.* (7) found that furosemide and furosemide esters were highly unstable when exposed to artificial laboratory light or daylight. These authors postulated, according to Moore and Sithipitaks (6), that the most likely photoreaction is dechlorination to give *N*-furfuryl-5-sulfamoylanthranilic acid and the corresponding esters.

In connection with a more detailed study of the photochemistry of furosemide in organic media, we note marked differences when photolysis was carried out in the presence and in the absence of oxygen. In these studies we found that the apparent rate constant for furosemide photodecomposition in methanol is about a factor 10 larger if irradiation is performed in the absence of oxygen. This difference would be explained in terms of an efficient quenching of the triplet state of the molecule, thus accounting for the effectivity of furosemide in photosensitized oxidation reactions in methanol (5). The same molecule shows a low, but biologically significant, quantum yield of singlet oxygen when furosemide-sensitized production of singlet oxygen at 1270 nm is observed. In addition to the photosensitizing ability of furosemide, this molecule reacts efficiently with excited molecular oxygen.

In this work we report on kinetic results obtained in the study of the sensitized photo-oxidation of furosemide using both steady-state and time-resolved methods. Additionally, product identification and solvent effect correlations were employed to propose a reaction mechanism.

MATERIALS AND METHODS

The following compounds: furosemide (Sigma Chemical Co.), phenazine, rubrene, 5,10,15,20-tetraphenyl-21H,23H-porphine (TPP) and 9,10-dimethylanthracene (DMA) (Aldrich Chemical Co.) were used without further purification. Furfurylamine, 2-methylfurane and benzophenone (Aldrich Chemical Co.) were distilled twice prior to use. All solvents used (Merck) were spectroscopic or HPLC quality.

Ultraviolet–visible absorption spectra and steady-state competitive kinetic experiments were performed in a Unicam UV-4 spectrophotometer interfaced with a DTK personal computer. The cell holder was maintained at 22.0 ± 0.5°C by circulating water from a Haake thermoregulated bath.

Chemical reaction rate constants were determined using a double wall cell of 10 mL capacity, light protected by black paint. A cen-

*Dedicated to the memory of Juan José Cosa.

†To whom correspondence should be addresed at: Universidad de Chile, Facultad de Químicas y Farmacéuticas, Departamento de Química Orgánica y Fisicoquímica, Casilla 233, Santiago 1, Santiago, Chile. Fax: 56-2-6782809; e-mail:azanocco@ll.ciq.uchile.cl

‡*Abbreviations:* DMA, 9,10-dimethylanthracene; furosemide, 4-chloro-*N*-furfuryl-5-sulfamoylanthranilic acid; TPP, 5, 10, 15, 20-tetraphenyl-21H, 23H-porphine.

tered window allows irradiation with light of a given wavelength by using Schott cut-off filters. The cell was thermostated by circulating water at 22.0 ± 0.5°C. The TPP (λ_{max} = 419 nm) was employed as a sensitizer. Illumination was performed with a visible, 200 W, Par lamp. In these experiments furosemide consumption was evaluated by observing the decrease in the concentration of the substrate in a Waters 600 HPLC system equipped with a Waters 474 fluorescence detector ($\lambda_{exc.}$ = 286 nm, $\lambda_{em.}$ = 410 nm) and a Merck RP Select B column. A linear gradient from methanol–1% aqueous acetic acid (1:9) to 100% methanol in 7 min was used to elute the samples. 9,10-Dimethylanthracene was employed to evaluate the steady-state concentration of $O_2(^1\Delta_g)$ (8).

Time-resolved phosphorescence measurements were carried out in 1 cm fluorescence cuvettes. Phenazine excitation was by absorption of the third harmonic (355 nm, ~15 mJ per pulse) of the 6 ns light pulse of a Quantel Brilliant Q-switched Nd:YAG laser. When TPP was used as the sensitizer, excitation was by absorption of the 500 ps light pulse of a PTI model PL-202 dye laser (419 nm, ~200 μJ per pulse). A PTI model PL-2300 nitrogen laser was employed to pump the dye laser. A liquid nitrogen-cooled North Coast model EO-817P germanium photodiode detector, equipped with a built-in preamplifier was used to detect infrared radiation emitted from the cuvette. The detector was coupled to the cuvette in right-angle geometry. The only elements between the cuvette face and the diode cover plate were an interference filter (1270 nm, Spectrogon US, Inc.) and a cut-off filter (995 nm, Andover Corp.). The output of the preamplifier was fed into the 1 MΩ input of a digitizing oscilloscope Hewlett Packard model 54540 A. Computerized experiment control, data acquisition and analysis were performed by a LabView-based software developed in our laboratory. Singlet oxygen quantum yields (Φ_Δ) were measured in time-resolved phosphorescence experiments using benzophenone as the actinometer (Φ_Δ = 0.37 in acetonitrile, Φ_Δ = 0.31 in benzene) (9), by comparing the response of the detector extrapolated at zero time and zero laser power, the latter adjusted using a set of neutral density filters.

Electronic impact mass spectra were obtained in a Fisons MD-800 gas chromatography/mass spectrometry system equipped with a Hewlett Packard Ultra-2 (25 m) capillary column or in a Fisons Platfform II mass spectrometer interfaced to a Hewlett Packard 1050 HPLC system. The NMR experiments were performed in a Bruker ADX 300 NMR spectrometer.

Oxygen consumption experiments were carried out in a double-wall cell of 10 mL capacity, light-protected by black paint. A centered window allows irradiation with light of a given wavelength by using a Schott cut-off filter. Oxygen concentration in methanol was continuously monitored using a Clark-type electrode attached to a YSI model 58 dissolved oxygen meter.

Peroxide measurements were performed using Mair and Graupner's method (10) that involves volumetric determination of the iodine liberated by the redox reaction between iodide and peroxide.

Simple semiempirical calculations of charge distribution in furosemide were performed employing the MOPAC 6.0 program, working in cartesian coordinates. Geometry optimization and calculations were performed using the AM1 method. The X-ray diffraction data were employed to introduce initial geometry parameters.

Low molecular weight products of furosemide photooxidation in methanol were isolated by solvent evaporation under nitrogen. Solid residue was extracted with benzene followed by solvent elimination under nitrogen and recrystallization of the solid product from carbon tetrachloride.

RESULTS AND DISCUSSION

Generation of singlet oxygen by furosemide

Direct evidence of $O_2(^1\Delta_g)$ generation by furosemide was demonstrated for the first time by detection of $O_2(^1\Delta_g)$ phosphorescence emission, λ_{max} = 1270 nm, following laser excitation at 355 nm (Nd–Yag laser). This method is much more reliable than the indirect trapping method with diphenylisobenzofuran; it may give erroneous results, if significant interactions between the sensitizer and the molecule under study occur (11). Using the phosphorescence method (12),

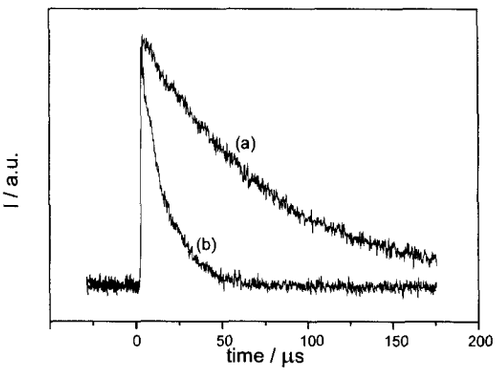

Figure 1. a: Singlet oxygen phosphorescence decay at 1270 nm, following dye laser excitation at 419 nm, using TPP as sensitizer in acetonitrile as the solvent. b: As in a, but in the presence of 0.54 m*M* furosemide.

quantum yields (Φ_Δ) equal to 0.047 ± 0.003 and 0.078 ± 0.004 were determined for $O_2(^1\Delta_g)$ formation by furosemide photosensitization in acetonitrile and benzene, respectively. These values were independent of furosemide concentration, between 1.5×10^{-2} and 8×10^{-2} m*M*. Furthermore, these values were independent of the laser power, between 4 and 45 mJ per pulse. Using phase demodulation methods, fluorescence lifetimes of furosemide equal to 950 ± 60 ps, 880 ± 52 ps and 990 ± 58 ps were determined in nitrogen-saturated solutions of furosemide in methanol, acetonitrile and benzene, respectively. Similar values within the experimental error were obtained in air-saturated solutions in the same solvents. These results show that no appreciable quenching of furosemide excited singlet state occurs in these conditions and suggest that singlet oxygen generation by furosemide involves triplet quenching of the drug. In spite of the low Φ_Δ observed values, these could explain, at least partially, photodynamic action of furosemide (1).

Reaction of furosemide with singlet oxygen

In most of the solvents employed in this work, total rate constants, k_T, for the reaction between furosemide and $O_2(^1\Delta_g)$, were determined using time-resolved phosphorescence measurements. Figure 1 shows the luminescence decay of singlet molecular oxygen at 1270 nm in acetonitrile as the solvent and TTP as the sensitizer. In the same figure the decay obtained in the presence of 0.54 m*M* of furosemide is included. From the single exponential decays, the lifetime of $O_2(^1\Delta_g)$ in the absence and in the presence of variable concentrations of furosemide was obtained. If decay data are represented according to Eq. 1, linear plots in the range of furosemide concentrations employed are obtained.

$$\tau^{-1} = \tau_o^{-1} + k_T\,[\text{furosemide}]. \qquad (1)$$

Figure 2 shows a typical Stern–Volmer-type plot for the quenching of singlet molecular oxygen by furosemide. Total rate constants, k_T, in different solvents, for the reaction between furosemide and $O_2(^1\Delta_g)$ were obtained from the slope of these plots. When water, chloroethanol and formamide were the solvents, phenazine was used as a sensitizer.

Due to the low solubility of furosemide in benzene (smaller than 1.2 m*M*), no reliable quenching data of $O_2(^1\Delta_g)$ by

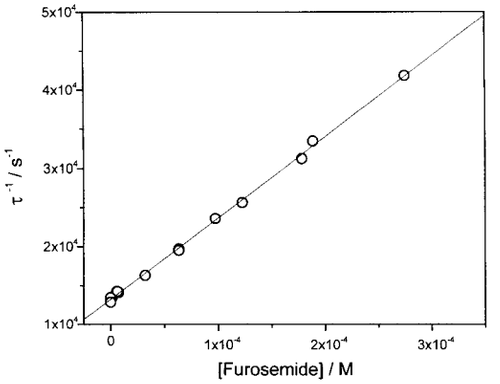

Figure 2. Stern–Volmer-type plot for the deactivation of singlet oxygen by furosemide in acetonitrile.

furosemide were obtained. In this solvent, values of k_T were determined by observing the inhibition of the rubrene autooxidation rate at 520 nm. In this case kinetics does not correspond to first order and the rate constant was obtained from the initial rates of rubrene consumption (13) according to Eq. 2:

$$k_T = \frac{k_d + k_{ox}[R]_o}{[F]}\left[\frac{(\partial[R]/\partial t)_i}{(\partial[R]/\partial t)_i^F} - 1\right] \quad (2)$$

where $[R]_o$ and [F] are the initial rubrene and furosemide concentrations, $(\partial[R]/\partial t)_i$ and $(\partial[R]/\partial t)_i^F$ are the initial consumption rates of rubrene in the absence and in the presence of furosemide and k_d and k_{ox} are the rate constants for the decay of singlet molecular oxygen in the solvent and the reaction rate of rubrene with $O_2(^1\Delta_g)$, respectively. Table 1 includes the values of k_T determined in different solvents.

Regardless of the sensitizer employed to evaluate k_T, these methods are applicable only if furosemide does not quench the sensitizer excited states, singlet or triplet under the experimental conditions employed (14). We can disregard this possibility for the following reasons: (1) in steady-state experiments, values of k_T were found independent of the initial concentration of rubrene; (2) linear Stern–Volmer-type plots were obtained over a wide range of furosemide concentrations (to 40 m*M*); (3) very close values of k_T, 3.2×10^7 M^{-1} s^{-1} and 2.5×10^7 M^{-1} s^{-1} were obtained in the mixtures benzene : methanol (2:1) and benzene : methanol-d_4 (2:1), respectively (15) and (4) sensitizer consumption was not observed in time-resolved measurements.

The rate constants for the chemical reaction between furosemide and $O_2(^1\Delta_g)$ were determined in acetonitrile, benzene and methanol employing TPP as sensitizer. Furosemide consumption was evaluated by observing the decrease in concentration of the drug as a function of the reaction time. To determine the steady-state $O_2(^1\Delta_g)$ concentration, DMA was used as an actinometer (8). Rate constants for chemical reaction, k_R, were obtained from the slope of pseudo-first-order plots. These results are included in Table 1.

Values of k_R are very similar to those obtained for k_T in the same solvent, indicating that most of the encounter complexes resulting from the interaction between furosemide and singlet oxygen evolve to yield products. Furthermore, although total rate constant values for the quenching of singlet

Table 1. Values of k_T and k_R for the reactions between furosemide, 2-methylfurane and furfurylamine with $O_2(^1\Delta_g)$ in different solvents

Solvent	$k_R/10^7$ M^{-1} s^{-1} furosemide	$k_T/10^7$ M^{-1} s^{-1}		
		Furosemide	2-Methylfurane*	Furfurylamine*
1 Methanol	1.04 ± 0.05	1.16 ± 0.06*	11.60 ± 0.62	4.66 ± 0.22
2 Ethanol		1.63 ± 0.09*	8.28 ± 0.54	4.49 ± 0.27
3 *n*-Propanol		2.30 ± 0.14*	8.82 ± 0.69	4.20 ± 0.23
4 *n*-Butanol		2.00 ± 0.13*	7.31 ± 0.37	4.05 ± 0.21
5 *n*-Pentanol		2.10 ± 0.11*		
6 *n*-Octanol		2.00 ± 0.10*	7.20 ± 0.35	4.24 ± 0.24
7 *i*-Propanol		1.96 ± 0.30*		3.95 ± 0.24
8 Cyclohexanol		7.31 ± 0.38*	9.41 ± 0.49	4.67 ± 0.28
9 *n*-Hexanol			7.48 ± 0.41	13.70 ± 0.82
10 Bencylic alcohol		7.62 ± 0.41*	24.10 ± 1.45	11.60 ± 0.61
11 Ethylenglycol			14.20 ± 0.82	4.46 ± 0.24
12 Benzene	1.06 ± 0.1	1.67 ± 0.08†	12.20 ± 0.62	7.49 ± 0.52
13 *n*-Hexane			2.51 ± 0.13	1.69 ± 0.08
14 Chloroform		1.80 ± 0.09*		
15 Methylene chloride		2.85 ± 0.15*	11.10 ± 0.58	6.30 ± 0.33
16 Acetone		3.93 ± 0.16*	13.90 ± 0.71	8.49 ± 0.45
17 Dimethylformamide		8.08 ± 0.42*	28.40 ± 1.53	20.50 ± 1.23
18 Acetonitrile	3.5 ± 0.4	5.24 ± 0.21*	18.80 ± 1.01	10.00 ± 0.58
19 Benzonitrile			20.20 ± 1.04	
20 Formamide		9.46 ± 0.40‡		
21 Ethyl acetate		3.50 ± 0.18*	9.79 ± 0.51	8.69 ± 0.42
22 2-Chloroethanol		25.8 ± 1.30‡	22.40 ± 1.15	
23 Water, pH 10		28.9 ± 1.42‡		
24 Propylencarbonate			29.00 ± 1.62	20.30 ± 1.02

* Sensitizer: TPP, dye laser; Nd-YAG laser.
† Sensitizer: rubrene, steady-state method.
‡ Sensitizer: phenazine, Nd-YAG laser.

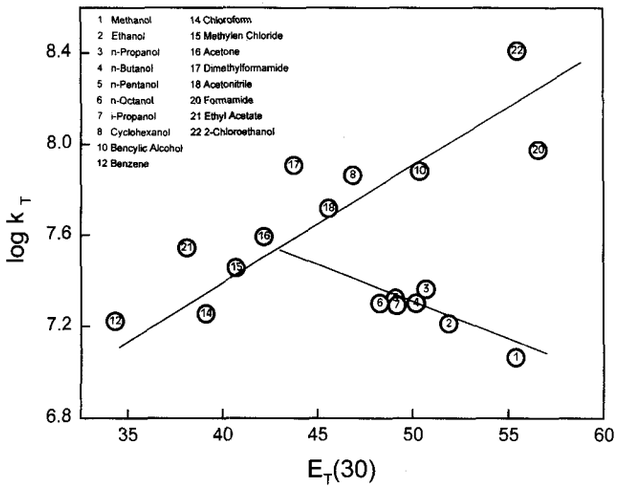

Figure 3. Plot of log k_T *versus* $E_T(30)$ for the reaction between furosemide and singlet oxygen.

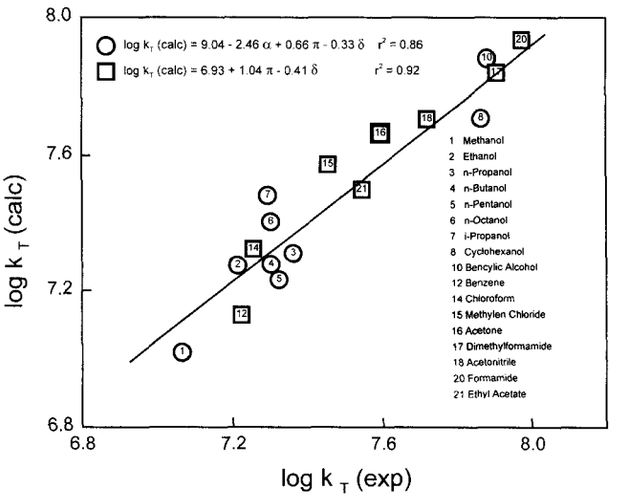

Figure 4. Plot of log k_T (calculated) *versus* log k_T (experimental) for the reaction between furosemide and singlet oxygen: (□) nonprotic solvents; (○) aliphatic alcohols.

oxygen by furosemide are solvent dependent as shown in Table 1, increasing from $1.7 \times 10^7\ M^{-1}\ s^{-1}$ in benzene to $28.9 \times 10^7\ M^{-1}\ s^{-1}$ in water at pH 10, the nature of the encounter complex cannot be suggested from a simple analysis of the dependence of k_T on macroscopic solvent parameters such as the dielectric constant, ϵ. For instance, in chloroform ($\epsilon = 32.66$), the k_T value is very close to those determined in benzene ($\epsilon = 2.27$).

Taking furosemide molecular structure into account, there are at least two possible sites that can suffer the attack of singlet oxygen, the nitrogen atom in the secondary amine group and the furane ring. A rough first approach to estimate the relative importance of each site was obtained from simple semiempirical calculations of charge distribution in furosemide employing the MOPAC-AM1 program and using X-ray diffraction data (16) to introduce the optimal geometry. From these calculations, it was found that the relative charge density on the nitrogen atom in the secondary amino group is approximately a factor two larger than the one calculated for carbons in the furane ring. This result suggests that the main path for the reaction between furosemide and singlet oxygen could involve the interaction of $O_2(^1\Delta_g)$ with the secondary amine group to generate a charge transfer intermediate, followed by product formation. However, k_T values in several solvents are on the order of those reported in the literature for the reactions between singlet oxygen with both aliphatic amines and substituted furanes (17–20), which precludes the obtention of additional conclusions about the reaction site in the furosemide molecule.

In order to clarify the nature of the reaction and its mechanism, an analysis of solvent effects in terms of multiparametric correlations using microscopic solvent parameters was performed. No good fittings were obtained when data were correlated using a generalizated solvatochromic equation (21,22). However, plots of log k_T *versus* the solvent parameter $E_T(30)$, as shown in Fig. 3, exhibit a clear dependence of k_T on the $E_T(30)$ parameter at least in nonprotic solvents. This result indicates that there is a significant charge separation along the reaction coordinate, and the intermediate is stabilized in polar solvents. Additionally, as can be noted in Fig. 3, aliphatic alcohols separate markedly from the main tendency. In this type of solvent, k_T diminishes with greater values of $E_T(30)$, a result that suggests a different effect of this type of solvent on the stabilization of the activated complex. If k_T values obtained in nonprotic solvents and the ones obtained in aliphatic alcohols are correlated separately using a generalized solvatochromic equation (21,22), the behavior shown in Fig. 4 is observed. In nonprotic solvents, k_T is dependent only on the π parameter, while in aliphatic alcohols k_T values depend on parameters α and π. These results can be understood if solvent effects on the sensitized photooxidation of triethylamine and asymmetrically substituted furanes, as 2-methylfurane and furfurylamine, are considered. Values of k_T for the reaction between 2-methylfurane and furfurylamine with $O_2(^1\Delta_g)$ measured in time-resolved experiences are included in Table 1. As is observed, the values for the reaction between singlet oxygen and these compounds also are solvent dependent but in a different way from that observed for furosemide. Table 2 includes characteristic coefficients associated with the solvent parameters when a generalized solvatochromic equation (21,22), appropriately modified, was employed to correlate experimental k_T values with microscopic solvent properties. The same table includes data obtained for triethylamine employed as a model tertiary amine (A. L. Zanocco, unpublished data).

Analysis of data in Table 2 allows the differences observed for k_T dependence in aliphatic alcohols and nonprotic solvents to be explained. As can be seen in this table, k_T values for furosemide in protic solvents are mainly sensitive to parameters α and π^*, with coefficients of -2.46 and 0.66, respectively. This dependence on solvent parameters is comparable to the one observed for triethylamine. As α takes into account the solvent ability to donate a hydrogen atom, it is obvious that solvents with the largest values of α diminished the reaction rate, preventing access of the excited oxygen to the reactive center in the furosemide molecule. This supports the idea that the reactive site in aliphatic alcohols corresponds to the secondary amino group. The

Table 2. Dependence of k_T values with microscopic solvent parameters for the reactions of furosemide, 2-methylfurane, furfurylamine and triethylamine with singlet oxygen

Compound	Log k_O	α	π^*	δ	r^2	n
Furosemide, aliphatic alcohols	9.04	−2.46	0.66	−0.33	0.86	9
Furosemide, nonprotic solvents	6.93	—	1.04	−0.41	0.92	8
2-Methylfurane	7.43	—	1.07	−0.09	0.90	17
Furfurylamine	7.32	−0.26	1.06	−0.12	0.95	17
Triethylamine	8.13	−1.23	0.35	−0.87	0.89	20

above considerations can be rationalized in terms of a mechanism involving the formation of a charge transfer complex (17,18) by the attack of excited oxygen to the nitrogen atom on the secondary amine group. This intermediate subsequently evolves to yield reaction products. Moreover, measurements of oxygen consumption in methanol show that the ratio between moles of oxygen consumed to moles of furosemide consumed increases with the photooxidation time range from 0.9 to 1.2 (until 30% furosemide consumption) up to 1.3 to 1.6 (at 80% reaction). This result suggests that addition of a second singlet oxygen molecule to the primary photooxidation product occurs. Scheme 1 presents the most probable mechanism for this reaction in aliphatic alcohols regarding the above observations.

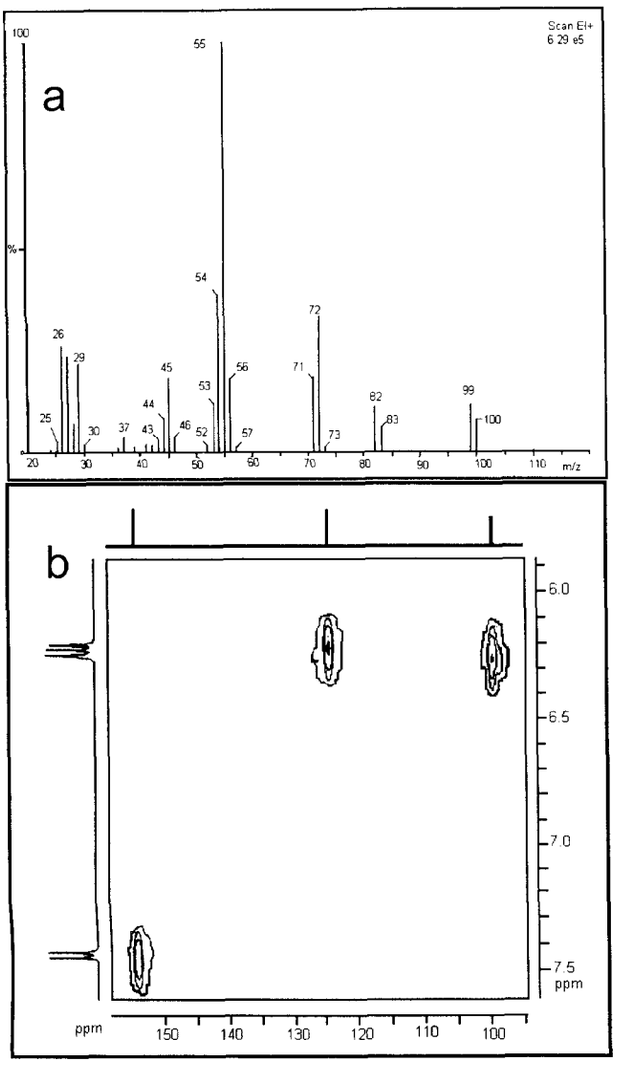

Figure 5. a: Electronic impact mass spectrum of butenolide 2. b: Proton–carbon correlation NMR spectrum of butenolide 2 in deuteroacetone as the solvent.

Scheme 1

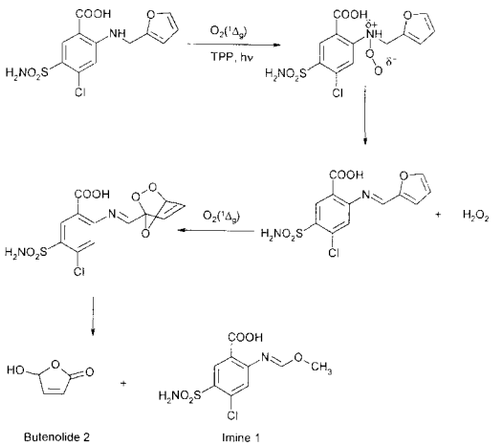

Additional support for the proposed mechanisms was obtained from the analysis of reaction products using mass spectrometry and ^{1}H-NMR. Figure 5 shows the mass spectrum and the HC correlation NMR spectrum obtained for only the low molecular weight product isolated in the photooxidation of furosemide in methanol using TPP as a sensitizer. Figure 5a shows a molecular ion at m/z equal to 100 and a fragmentation pattern that is compatible with the structure of butenolide 2. The HC correlation NMR spectrum of Fig. 5b shows that the doublet at 7.44 ppm correlates with a ^{13}C-NMR signal at 153.93 ppm, the singlet at 6.25 ppm correlates with a ^{13}C-NMR signal at 99.66 ppm and the doublet at 6.22 ppm correlates with a ^{13}C-NMR signal at 124.43 ppm. These can be ascribed to the olefinic proton on carbon 3, to the proton neighbor to the hydroxylic group and to the olefinic proton adjacent to the carbonyl group in the butenolide 2, respectively. An additional signal in the ^{13}C-NMR spectrum at 171.45 ppm can be attributed to the carbon atom of the carbonyl group. In these experiments, we were not able to isolate pure products coming from the aromatic moiety of furosemide. However, the ^{1}H-NMR spectrum of a partially purified product mixture shows a signal at 3.21 ppm, indicating the incorporation of a methoxyl group in the

product. Figure 6 shows the changes in the ^{1}H-NMR spectrum, between 6 and 8 ppm, as a function of photooxidation time (in CD_3OD as the solvent). The growths of signals corresponding to the butenolide 2 are clearly evident. Furthermore the formation of the imine derivative 1 can be supported by the growth of a singlet signal at 7.15 ppm. The chemical shift of this signal is within the range reported for similar imine compounds (23). Treatment of the crude reaction with an aqueous acid solution yields saluamine (as shown by its NMR and mass spectra) as the only aromatic product in the furosemide photooxidation. Formation of saluamine is easily explained by the hydrolysis of imine 1. Attempts to measure hydrogen peroxide formation using Mair and Graupner's method (10) permit us to detect only trace amounts (nonstoichiometric) of this product. Probably because this method requires large photooxidation times to accumulate measurable quantities of peroxide, side reactions involving hydrogen peroxide would occur under our experimental conditions.

In nonprotic solvents, k_T for furosemide is mainly dependent on the π^* parameter. As seen in Table 2, k_T for furosemide in nonalcoholic solvents does not depend on the α parameter and is mainly sensitive to the π^* parameter, a behavior very similar to that observed for 2-methylfurane and furfurylamine. Values of the coefficient associated with π^* are equal to 1.04, 1.07 and 1.06 for furosemide, 2-methylfurane and furfurylamine, respectively, a result that can be explained if the same reaction mechanism applies to the three molecules under consideration. If this dependence upon the solvent and classical 2 + 4 cycloaddition of singlet oxygen and furans (24) is considered, products arising from the reaction of singlet oxygen with the furane ring in the furosemide molecule can be represented according to Scheme 2.

Scheme 2

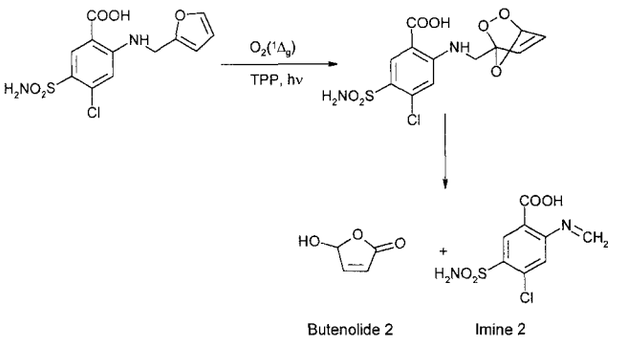

It should be considered that oxygen consumption measurements in acetonitrile give approximately a 1:1 relation of moles of furosemide consumed to moles of oxygen consumed even at a higher furosemide conversion.

Formation of butenolide 2 was demonstrated in the same form as described for reaction product analysis in aliphatic alcohols. Imine 2 was not isolated as a pure product, but the ^{1}H-NMR spectrum of the reaction products, partially purified in the absence of water, show a doublet at 5.29 ppm assigned to the iminic protons of the imine 2. Treatment of the crude reaction with water at pH 2, affords saluamine (characterized by its mass and ^{1}H-NMR spectra) as expected from the hydrolysis of imine 2.

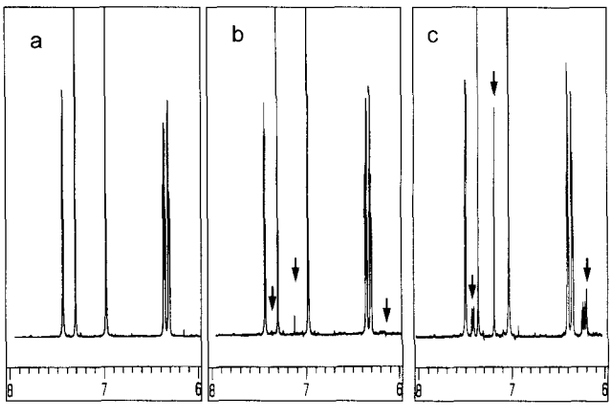

Figure 6. The ^{1}H-NMR spectrum between 6 and 8 ppm as a function of the photooxidation time of furosemide in CD_3OD as the solvent. Arrows show the growth of signal corresponding to the butenolide 2 and imine 1. (a) Time zero, (b) 20% of furosemide consumption and (c) 40% furosemide consumption.

Data obtained in this study show that the solvent activates one or the other of the two different furosemide sites available for attack by singlet oxygen. These significant differences can be explained if, in nonprotic solvents, the carboxylic substituent in the aromatic ring of furosemide interacts with the amino group to form intramolecular hydrogen bonding between the carboxylic oxygen and the hydrogen of amino group. Alternatively, intramolecular hydrogen bonding may occur between the hydroxylic proton and the nitrogen atom of the amino group. According to the MOPAC-AM1 simple calculations (solvent effects not included), there are no significant differences between the formation heats for one or the other hydrogen-bonding interactions. Then, if the electron pair on the nitrogen atom is occupied by intramolecular interactions, the attack of singlet oxygen is unfavorable and a reaction with the furane ring occurs. In aliphatic alcohols, solvation of the carboxylic group leaves the electron pair on the nitrogen atom available, and then the electrophilic attack of excited oxygen predominates.

CONCLUSIONS

Furosemide reacts efficiently with $O_2(^1\Delta_g)$. The reaction mechanism is strongly dependent on the solvent in which the photooxidation reaction is performed. In nonprotic solvents the reaction occurs predominantly by a 2 + 4 cycloaddition mechanism, whereas in aliphatic alcohols the interaction between singlet oxygen and the amino group in the furosemide molecule through the formation of a charge transfer intermediate appears as highly favorable. Additionally, data obtained in this study show that the furosemide photodynamic action can be related, at least partially, to the ability of furosemide to produce biologically significant quantities of singlet oxygen ($^1\Delta_g$) in polar and nonpolar media. Several authors have proposed that adverse photosensitivity effects of furosemide can be related to photoproducts arising from direct photolysis or those coming from type I photoreactions. Data obtained in this study suggest that photooxidation products, of similar structure to those obtained

by direct photolysis or in type I photoreactions, also should be responsible for the reported adverse photosensitivity of the diuretic.

Acknowledgements—The financial support from FONDECYT (grants 1940461 and 2950077) and DTI-University of Chile (grants Q3338-9322 and 10494) and the technical assistance of Mrs. Fresia Pérez are gratefully acknowledged.

REFERENCES

1. Magnus, I. A. (1976) *Dermatological Photobiology*, pp. 213–216. Blackwells, London.
2. Moore, D. E. (1977) Photosensitization by drugs. *J. Pharm. Sci.* **66**, 1282–1284.
3. Moore, D. E. and C. D. Burt (1981) Photosensitization by drugs in surfactant solutions. *Photochem. Photobiol.* **34**, 431–439.
4. Rowbotham, P. C., J. B. Stanford and J. K. Sudgen (1976) Some aspects of the photochemical degradation of frusemide. *Pharm. Acta Helv.* **51**, 304–307.
5. Moore, D. E. and S. R. Tamat (1980) Photosensitization by drugs: photolysis of some chlorine-containing drugs. *J. Pharm. Pharmacol.* **32**, 172–177.
6. Moore, D. E. and V. Sithipitaks (1983) Photolytic degradation of frusemide. *J. Pharm. Pharmacol.* **35**, 489–493.
7. Bungaard, H., T. Nǿrgaad and N. M. Nielsen (1988) Photodegradation and hydrolysis of furosemide and furosemide esters in aqueous solutions. *Int. J. Pharm.* **42**, 217–224.
8. Usui, Y., T. Michio and H. Nakamura (1978) Kinetic studies of photosensitized oxygenation by singlet oxygen in aqueous micellar solutions. *Bull. Chem. Soc. Jpn.* **51**, 379–384.
9. Wilkinson, F., W. P. Helman and A. B. Ross (1993) Quantum yields for the photosensitizing formation of the lowest electronically excited singlet state of molecular oxygen in solution. *J. Phys. Chem. Ref. Data* **22**, 113–262.
10. Mair, R. D. and A. J. Graupner (1964) Determination of organic peroxides by iodine liberation procedures. *Anal. Chem.* **36**, 194–204.
11. Tanielian, C. and C. Wolff (1995) Porphyrin-sensitized generation of singlet molecular oxygen: comparison of steady-state and time resolved methods. *J. Phys. Chem.* **99**, 9825–9830.
12. Scaiano, J. C., R. W. Redmond, B. Mehta and J. T. Arnanson (1990) Efficiency of the photoprocesses leading to singlet oxygen ($^1\Delta_g$) generation by α-terthienyl: optical absorption, optoacoustic calorimetry and infrared luminescence studies. *Photochem. Photobiol.* **52**, 655–659.
13. Carlsson, D. J., G. D. Mendenhall, T. Suprunchuk and D. M. Wiles (1972) Singlet oxygen ($^1\Delta_g$) quenching in the liquid phase by metal(II) chelates. *J. Am. Chem. Soc.* **94**, 8960–8962.
14. Davidson, R. S. and K. R. Trethewey (1977) Concerning the use of amines as probes for participation of singlet oxygen in dye-sensitised oxygenation reactions. *J. Chem. Soc. Perkin Trans. II*, 178–182.
15. Rodgers, M. A. J. (1983) Solvent-induced deactivation of singlet oxygen: additivity relationships in nonaromatic solvents. *J. Am. Chem. Soc.* **105**, 6201–6205.
16. Lamotte, P. J., H. Campsteyn, L. Dupont and M. Vermeire (1978) Structure cristalline et moléculaire de l'acide furfurylamino-2-chloro-4-sulfamoyl-5-benzoïque, la furosémide ($C_{12}H_{11}ClN_2O_5S$). *Acta Crystallogr.* **B34**, 1657–1661.
17. Encinas, M. V., E. Lemp and E. A. Lissi (1987) Interaction of singlet oxygen [$O_2(^1\Delta_g)$] with aliphatic amines and hydroxylamines. *J. Chem. Soc. Perkin Trans. II*, pp. 1125–1127.
18. Lissi, E. A., M. V. Encinas, E. Lemp and M. A. Rubio (1993) Singlet oxygen $O_2(^1\Delta_g)$ bimolecular processes. Solvent and compartmentalization effects. *Chem. Rev.* **93**, 699–723.
19. Gollnick, K. and A. Griesbeck (1985) Singlet oxygen photooxygenation of furans. *Tetrahedron* **41**, 2057–2068.
20. Clennan, E. L. (1991) Synthetic and mechanistic aspects of 1,3-diene photooxidation. *Tetrahedron* **47**, 1343–1382.
21. Reichardt, C. (1990) *Solvents and Solvent Effects in Organic Chemistry*. VCH, Weinheim.
22. Kamlet, M. J., J. L. M. Abboud, M. H. Abraham and R. W. Taft (1983) *J. Org. Chem.* **48**, 2877–2887.
23. Pretsch, E., T. Clerc, J. Seibl and W. Simon (1989) In *Tables of Spectral Data for Structure Determination of Organic Compounds* (Edited by F. L. Boschke, W. Fresenius, J. F. K. Huber, E. Pungor, G. A. Rechnitz, W. Simon, T. S West). H175, H180 Springer-Verlag, New York.
24. Clennan, E. L. (1991) Synthetic and mechanistic aspects of 1,3-diene photooxidation. *Tetrahedron* **47**, 1343–1382.